

# Acoustic Emission Signals in Thin Plates Produced by Impact Damage

William H. Prosser, Michael R. Gorman and Donald H. Humes

Received 30 June 1998. William H. Prosser and Donald H. Humes are affiliated with NASA Langley Research Center, Hampton, VA 23681-0001, and Michael R. Gorman is with Digital Wave Corp., Englewood, CO 80111

Journal of Acoustic Emission, Vol. 17(1-2), (June, 1999), pp. 29-36.

## Abstract

Acoustic emission (AE) signals created by impact sources in thin aluminum and graphite/epoxy composite plates were analyzed. Two different impact velocity regimes were studied. Low-velocity (less than 0.21 km/s) impacts were created with an airgun firing spherical steel projectiles (4.5 mm diameter). High-velocity (1.8 to 7 km/s) impacts were generated with a two-stage light-gas gun firing small cylindrical nylon projectiles (1.5 mm diameter). Both the impact velocity and impact angle were varied. The impacts did not penetrate the aluminum plates at either low or high velocities. For high-velocity impacts in composites, there were both impacts that fully penetrated the plate as well as impacts that did not. All impacts generated very large amplitude AE signals (1-5 V at the sensor), which propagated as plate (extensional and/or flexural) modes. In the low-velocity impact studies, the signal was dominated by a large flexural mode with only a small extensional mode component detected. As the impact velocity was increased within the low velocity regime, the overall amplitudes of both the extensional and flexural modes increased. In addition, a relative increase in the amplitude of high-frequency components of the flexural mode was also observed. Signals caused by high-velocity impacts that did not penetrate the plate contained both a large extensional and flexural mode component of comparable amplitudes. The signals also contained components of much higher frequency and were easily differentiated from those caused by low-velocity impacts. An interesting

phenomenon was observed in that the large flexural mode component, seen in every other case, was absent from the signal when the impact particle fully penetrated through the composite plates.

## **1. Introduction**

Damage from impact is a serious hazard to aircraft and spacecraft. During takeoff and landing, impact threats include runway debris and birds. Ice created on spacecraft from the exposure of humid air to the cold of cryogenic propellants may break off during launch and cause impact damage. There are also numerous in-flight sources of impact damage including birds, projectiles used against military aircraft, and collisions with other aircraft or spacecraft. For spacecraft, there is another hazard, which is the impact of micrometeoroids and space debris. These on-orbit collisions occur at velocities exceeding 10 km/s, and at these velocities, even very small particles can create significant damage. The seriousness of the threat of this type of impact damage to spacecraft is reflected in the titles of two government reports; “Space Program: Space Debris is a Potential Threat to Space Station and Shuttle” (GAO, 1990) and “Space Station: Delays in Dealing with Space Debris May Reduce Safety and Increase Costs.” (GAO, 1992)

Acoustic emission (AE) monitoring has been proposed as one method for structural health monitoring to detect, locate, and assess impact damage. Lempriere (1987) and Nelson and Lempriere (1987) discussed such applications of AE for spacecraft. The advantages of such a monitoring system are that the number of post-flight inspections can be minimized or eliminated. This can lead to a tremendous cost savings while at the same time providing enhanced safety. For long-term orbiting space platforms such as the proposed Space Station, routine inspections for impact damage are particularly difficult. Extra-vehicular activity (EVA) is expensive and dangerous, and there are limited space-

tested tools and techniques for damage inspection and assessment. A recent example demonstrating this point is the inability to find the leak in a Mir Space Station Module, caused by a collision with another spacecraft, even after several EVA inspections.

In this research, AE signals from impact sources in plates were detected with broad band, high fidelity sensors and digitized for analysis. Impact events were studied in both isotropic aluminum, and anisotropic graphite/epoxy. Both materials are widely used on aircraft and spacecraft. Low-velocity impacts were created with a pump airgun, firing spherical steel projectiles at velocities less than 0.21 km/s. Varying the number of times the airgun was pumped made it possible to study the effect of velocity variation within the low velocity regime. The effect of the angle of the plate on the observed signal was also evaluated. High-velocity impacts were generated in these plates with a two-stage light-gas gun. The velocity was varied over the range of 1.8 to 7 km/s. A smaller nylon projectile was used. Again, the angle of impact was varied. For the composite materials, by varying the velocity in the high-velocity regime, impacts that fully penetrated the plate were produced as well as those that did not.

For all conditions of impact studied in this research in both the aluminum and graphite/epoxy composite plates, the detected AE signals were of very large amplitude. At the relatively short distances of propagation (less than 20 cm) in this work, attenuators, rather than preamplifiers, were used in some cases. This was necessary to reduce the signal amplitudes to a sufficiently low level for digitization. All signals contained propagating plate mode (extensional and/or flexural) components. Although location results are not presented in this paper, the large amplitude signals (and thus large signal-to-noise ratios) made it possible to obtain excellent impact location agreement with that measured directly on the plate.

For low-velocity impacts, the flexural plate mode was predominant. As the projectile velocity was increased within the low-velocity regime, the overall amplitude of the modes increased and the amplitude of higher frequency components in the flexural mode increased. Previous research (Gorman, 1990; Gorman and Prosser, 1991; Prosser, 1991) showed the effect of the direction of source motion on the relative amplitudes of plate modes. This was the motivation for varying the angle of impact. In contrast to the previous studies, no clear effect of varying the trajectory on the relative amplitude of plate modes was observed.

For high-velocity impacts, the extensional mode amplitude was much larger than for low-velocity impacts and comparable to that of the flexural mode. The signals contained much higher frequency content. Again, the effect of varying the impact angle produced no change in the relative amplitudes of the plate modes. The flexural mode was entirely absent in every case where full penetration of the composite plate occurred. Further study of this effect is warranted as this could provide a useful discriminator for the detection of spacecraft-hull penetration.

In previous research, attempts were made to use acoustic detectors to characterize the micrometeoroid environment. Examples of this work are described by Konstantinov et al. (1969), Alexander et al. (1962), and Kapinsinsky (1978). Laboratory experiments were used to characterize the sensitivity of the devices and such acoustic detectors were widely flown on balloons, sounding rockets, satellites, and lunar and deep-space probes. However, much like AE testing of structures, the reliability of the data from these on-board acoustic sensors has often been questioned because extraneous noise was not identified or eliminated. Thus, the rates of impacts determined from acoustic signals were unrealistically high in comparison to other measurement systems such as capacitive discharge detectors.

The extraneous noise signals were attributed to both electromagnetic interference and noise caused by thermal expansion of the spacecraft.

Laminated composite materials offer considerable weight savings for aircraft and spacecraft, but are particularly susceptible to impact damage. As such, there has been considerable study on acoustic waves generated by impact sources (Gardiner and Pearson, 1985; Weems et al., 1991; Takeda et al., 1981). However, these studies have focused primarily on impact sources of very low velocity such as dropped projectiles or weights dropped onto impact tups. The signals acquired in these experiments are in agreement with the results from the low-velocity impact testing in this study in that small amplitude extensional mode components followed by much larger flexural mode components can be identified. In addition, a number of authors including Moon (1973), Sun and Lai (1974), Datta et al. (1992), Karim (1991), and Mal and Lih (1992) have investigated theoretical approaches for predicting acoustic waves in composite laminates generated by impact sources.

More recently, Nelson and Lempriere (1987) evaluated AE signals generated by impact sources in metallic plates for the development of AE technology for the Space Station. Although they successfully demonstrated the detection and location of impacts, an AE monitoring system was not included in later plans for the Space Station. It is believed that the infant state of the waveform-based technology used, combined with severely limited development funds, led to the curtailment. In their study, they detected and digitized signals with broadband sensors for low-velocity impacts created with an air gun and spherical projectiles. They also collected signals from a very limited number of high-velocity impacts, but the results were not discussed in detail. AE signals propagating as plate modes were also observed in both cases and considerable discussion focused on the ability to locate sources with these dispersive waves. However, they tested only metal

specimens representative of space-station materials and only considered normal impact. They also suffered problems with their digitizing instrumentation causing high frequency spikes that distorted some signals. Furthermore, differences between penetrating and non-penetrating high-velocity impacts were not evaluated. Thus, a more extensive study was conducted and the results are detailed below.

## **2. Low-Velocity Impact**

A pump air gun (Daisy model 880) was used to produce low-velocity impacts. Spherical, steel balls with a diameter of 4.5 mm were used. The velocity of the projectiles was not measured in these experiments. The nominal maximum muzzle velocity for this model gun, as obtained from the manufacturer, is 0.21 km/s when the gun is pumped to its full capacity of 10 pumping. At this velocity, the estimated kinetic energy ( $mv^2/2$ ) of the projectile is 8.2 J.

The target plate was 2024 aluminum sheet with a thickness of 3.175 mm and 50.8 cm square. For safety, the target plate with attached sensors was placed inside a chamber of 76-mm thick high density foam. The plate was placed on a fixture that allowed the angle of impact to be varied from normal to the plate ( $90^\circ$ ) down to  $10^\circ$  grazing incidence in  $10^\circ$  steps.

Heavily damped, 3.5 MHz ultrasonic transducers for thickness gaging (Panametrics model V182) were used to detect the signals produced by these low-velocity impacts. Operated far off their resonance in the low-frequency AE range (less than 1 MHz), these sensors provide flat with frequency, high-fidelity, displacement response. This was demonstrated (Prosser, 1991) by comparison of their response against that of a calibrated laser interferometer. In addition, Papadakis (1980) discussed why such transducers make ideal high-fidelity AE sensors. This sensor has a diameter of 1.27 cm. This large aperture

leads to problems with phase cancellation across the sensor face at higher frequencies. To reduce this effect, a smaller diameter sensor (Digital Wave Corp., model B1025) was used in the high-velocity impact studies, which were conducted later. Even though these two sensors have similar response curves as a function of frequency except for the aperture effects, exact comparisons of the low- and high-velocity impact generated AE signals are not made. This is particularly true for the higher-frequency extensional mode and the higher-frequency component of the flexural mode. However, gross differences of these signals, particularly of the relative amplitudes of the plate modes between low-velocity and high-velocity impacts are noted and will be discussed.

For these experiments, four sensors were placed in a rectangular array around the anticipated impact spot. They were all located at a nominal distance of 15.2 cm from the impact. In repeated test firing, the impact position did not vary more than 1.27 cm in any direction from the desired impact position. As the amplitudes of the AE signals produced by these impacts were so large, no preamplifiers were used. The output of the sensors were put directly into a transient recorder (LeCroy model 6810) which had a 12-bit vertical resolution. A sampling frequency of 2 MHz was used and 1024 points were acquired for each waveform.

A typical signal captured from an impact, in which the gun had been pumped five times is shown in Fig. 1a. The extensional and flexural mode components of this signal

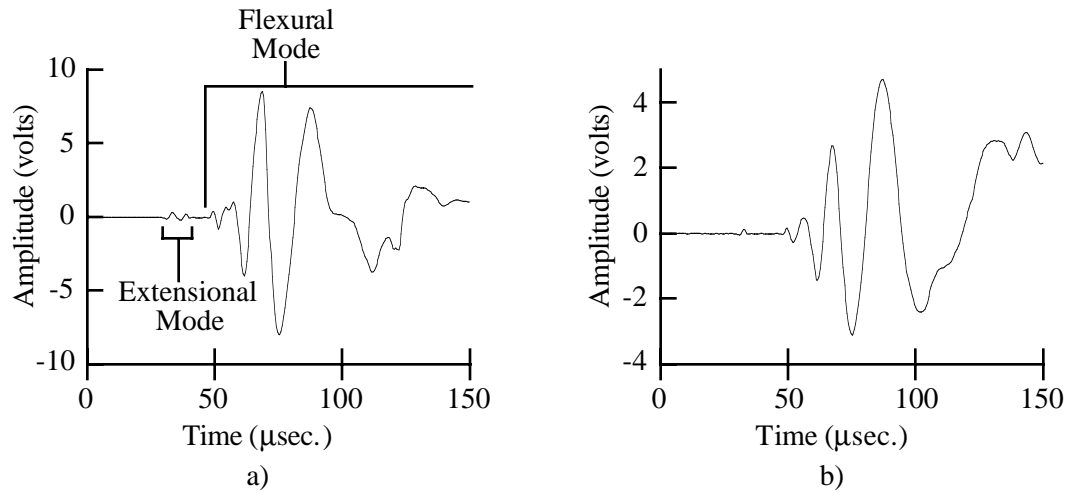


Fig. 1 AE signals produced by low-velocity impact on aluminum plate with: a) air gun pumped 5 times, and b) air gun pumped 2 times.

are identified in this figure. The extensional mode propagates with a faster velocity and suffers little dispersion, while the flexural mode travels more slowly with dispersion such that higher frequencies arrive earlier in the signal. The peak amplitude of the signal is quite large, and again, this is without any amplification. The flexural mode is dominant and the extensional mode is barely observable in comparison. This is as expected since the impact produces a large out-of-plane source motion and thus generates a large bending moment. For these impacts, the projectile did not penetrate the plate but did produce a significant crater. The crater diameter was approximately the same diameter as the spherical projectile.

A signal from an impact, in which the gun was only pumped twice is shown in Fig. 1b. The velocity (and energy) of the projectile for this case is smaller, which leads to a smaller peak amplitude. Again, the flexural mode is dominant with very little extensional mode signal present. Not only is the amplitude different for the signals from different impact velocities, but the frequency content changes as well. As can be seen in the time



domain signals of Fig. 1, and even more clearly in their frequency response curves in Fig. 2, the high-frequency content increased in the signal from the higher-velocity impact.

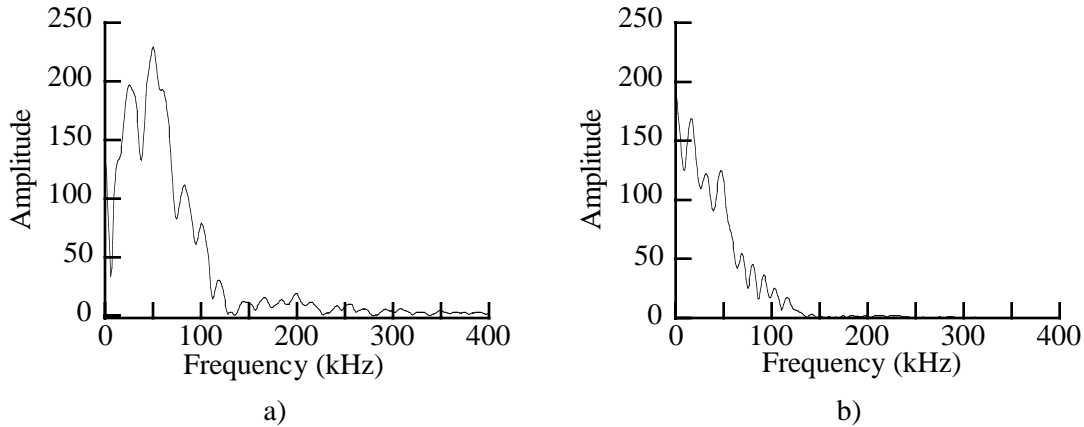


Fig. 2 Magnitude of FFT of AE signals in Fig. 1 produced by low-velocity impact on aluminum plate with: a) air gun pumped 5 times, and b) air gun pumped twice.

No effect of impact-angle variation on the relative amplitudes of the two plate modes was observed. As mentioned previously, earlier research (Gorman, 1990; Gorman and Prosser, 1991; Prosser, 1991) had demonstrated a strong relationship between the directionality of the source motion and the relative amplitudes of plate modes. In this previous work, the simulated AE sources (pencil-lead breaks) were all applied at the mid-plane of the plate as the source angle was varied. Impact sources, however, occur on, or near the surface of the plate. This off-mid-plane source always creates a large bending moment, and thus large flexural mode. The variation in the angle of impact produced frequency content and overall amplitude (of both modes) changes similar to those produced by varying the velocity. This is because the normal component of the impact velocity changes, as the angle is varied. These effects, as well as signal dispersion effects due to slight variation in the propagation distance from shot to shot, all contributed to further mask any possible effect on relative amplitudes of plate modes that might have been caused by

impact angle variations. Further study is needed to determine the feasibility of impact trajectory assessment through AE signal analysis.

### **3. High-Velocity Impact**

A two-stage light-gas gun was used for high-velocity impact experiments. These high-velocity impacts cause damage, which more closely simulates that caused by hypervelocity impacts of micrometeoroids and space debris on spacecraft.. The first stage of this gun consisted of a Swift 5.59-mm caliber rifle, which fires a nylon piston. The barrel for this first stage is pressurized with hydrogen prior to the shot. As the 5.59-mm diameter nylon piston is fired down the barrel in the first stage, it further compresses the hydrogen until the high pressure ruptures a polymer membrane at the muzzle end of the first stage. The piston is caught in a large steel capture block prior to reaching the end of the first stage. The pressurized hydrogen then propels a much smaller projectile down an evacuated chamber at velocities, for this gun, up to 7 km/s. More details about the operation of such guns are given by Crozier and Hume (1957) and more recently by Schneider and Stilp (1990).

The velocity is controlled by a number of factors including the projectile size and weight, the amount of powder charge in the first stage, and the original pressure of the hydrogen gas in this stage. For these experiments, the impact projectiles were nylon cylinders with diameter of 1.5 mm and length of 1.25 mm. The velocity was measured with an optical system. Using mirrors, the path of a He-Ne laser beam was manipulated so that it passed twice through the intended path of the projectile at known, fixed distances between passes. The laser beam then impinged on a photo-detector. As the impact projectile traveled down the chamber, each time it passed through the laser beam, it temporarily blocked the light from arriving at the photo-detector. The photo-dector output

signal could then be used to determine the time required for the particle to travel the distance between the two beam paths. This time, with the known distance, was then used to determine the velocity of the projectile, which in our experiments ranged from 1.8 to 7 km/s. Over this velocity range, the calculated kinetic energy of the projectile ranges from 4.1 J to 61.7 J. Thus, even though the velocities are much higher than those used in the low-velocity study, the energy of the projectile is of the same order of magnitude.

Both aluminum and graphite/epoxy composite plates were impacted at high velocities. The 2024 aluminum plates had the same nominal thickness and lateral dimensions as those used for low-velocity experiments. Two different graphite/epoxy composites were used. The first was 8 plies of IM7/8552, which had a nominal thickness of 1.27 mm. The lateral dimensions of these plates varied but was 25.4 x 25.4 cm or larger. The second was 24 plies of IM7/977-2 with a nominal thickness of 3.56 mm. The lateral dimensions of these plates were 35.6 x 35.6 cm. Both laminates were quasi-isotropic lay-ups, the first being  $[0, 45, 90, -45]_S$  and the second being  $[0, 45, 90, -45]_{3S}$ . For the composites, only impact normal to the plate was studied, while for the aluminum, the impact angle was varied again from normal ( $90^\circ$ ) down to  $10^\circ$  in  $10^\circ$  steps.

As mentioned previously, different sensors (Digital Wave Corp. model B1025) were used for the high-velocity experiments. These were similar to those used in the low-velocity impact study in that they are highly damped ultrasonic sensors operating far off resonance to provide a flat frequency response. However, they have a smaller diameter, which minimizes aperture effects thus providing better fidelity at the higher frequencies in the extensional mode and the early portion of the flexural mode. Again, four sensors were used in an array around the impact site. However, in this case, they were not equidistant from the impact site. For the aluminum plates, the nominal sensor positions were as shown in Fig. 3. For the composite plates, similar sensor spacing was maintained, but

because the lateral dimensions of the plate were different, the positions relative to the plate edges were different. Also, as illustrated in this figure, there was slightly larger variability of the impact site from shot to shot.

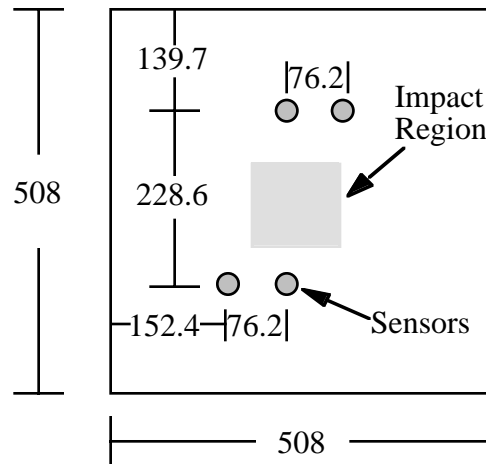


Fig. 3 Illustration of sensor positions for high-velocity impact in aluminum plate. Dimensions in mm.

A different signal recording system (Digital Wave Corp. model 4012 Fracture Wave Detector) was used for these experiments. It also had 12-bit vertical resolution, but the sampling frequency was 10 MHz. The signal was bandpass filtered from 20 kHz to 1.5 MHz. Because the input range of this digitizer was limited to  $\pm 0.5$  V, an attenuating preamplifier (Digital Wave Corp. model 2040 G/A) was used to provide 20-dB attenuation. For the signals presented in this paper, the amplitudes have been multiplied by 10 to correct for this attenuation and provide the voltage output from the sensor. This allows direct comparison of these signals against those recorded from the low-velocity impact study. However, the differences in type of sensors and filtering must be considered when making such comparisons. Thus, only significant differences in wave shape and modal content will be discussed between these two impact conditions.

Figure 4a shows the signal produced in an aluminum plate from a high-velocity impact. The velocity of the impact particle was 4.2 km/s and the aluminum plate was not penetrated. In fact, for the range of velocities tested, no projectiles penetrated the aluminum plates. The propagation distance to the sensor was 14.7 cm. Because of the significant high-frequency components in this signal, it is more difficult to clearly identify the extensional and flexural mode components. A 500 kHz low-pass filter was applied with the results shown in Fig. 4b. Here the plate mode components are more readily identified. In comparing these signals to the low-velocity impact signals in Fig. 1, it is noted that the shift in arrival times of these signals, and others to be presented later, are due to differences in trigger timing. Two significant differences are readily apparent when comparing signals caused by high-velocity impact to those caused by low-velocity impact. The first, which was clearly demonstrated by the need to use a low-pass filter to identify the modes, is that there is much higher frequency content in signals produced by high-velocity impact. It is suspected, although not verified by signal analysis, that higher order Lamb modes may be present in this high-frequency signal. This higher frequency content is not unexpected due to the source mechanism at much higher velocity. An increase in high-frequency content was also observed even for the slight velocity increase in low-velocity impact (cf. Fig. 2).

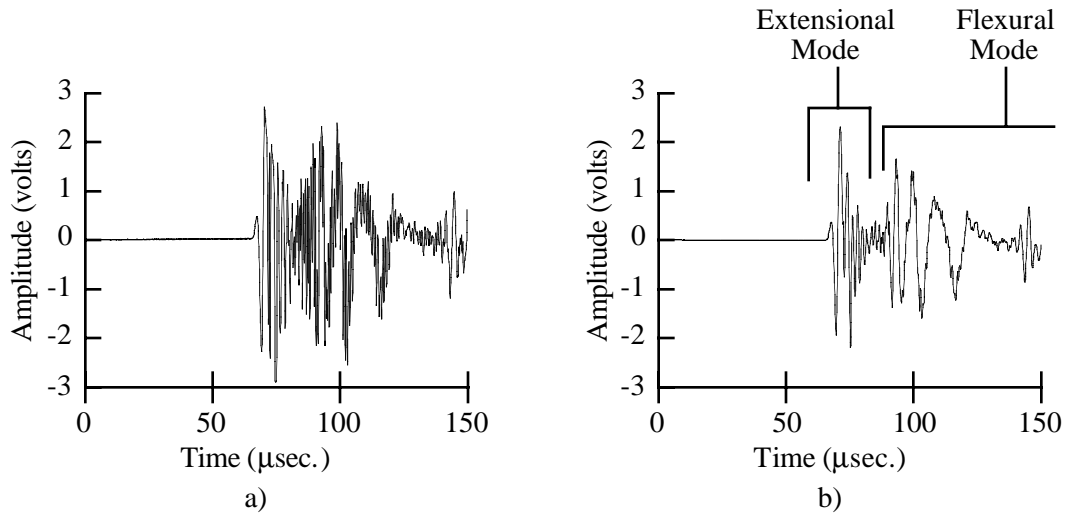


Fig. 4 a) AE signal produced by high velocity impact on aluminum plate; b) same signal as a) except after filtering with 500-kHz low-pass filter.

The second significant difference between the low- and high-velocity impact signals is the much larger extensional mode component for high-velocity impacts. It has an even larger amplitude than the flexural mode for this signal. A qualitative explanation for this difference can be offered based on an examination of the type of deformation produced by impacts at these different velocities. As discussed previously, low-velocity impact produces a crater, which is of similar diameter to the projectile diameter. For high-velocity impact, however, the diameter of the crater is several times larger than the diameter of the projectile. Thus, there is significant in-plane deformation as the crater expands in the high-velocity impact event. It seems likely that this in-plane deformation from crater expansion accounts for the large extensional plate mode component in high-velocity impact signals.

Again, no clear difference in the relative amplitude of the plate-mode components was detected as a function of the angle of impact. As the angle was decreased from normal impact, overall decreases in signal amplitude were observed as the normal component of the velocity decreased. However, the larger variations in the actual impact spot relative to

the sensor positions made it difficult to investigate this effect. The apparent amplitudes of the modes change with propagation distance, especially for the flexural mode because of its high dispersion. Further, more controlled tests, in which either the propagation distance varied less, or amplitude changes due to propagation distance variations are compensated, are required. This will allow a better determination of whether information about impact trajectory is also contained in AE signals.

For high-velocity impacts in composite plates, the impact projectile fully penetrated the plate in most cases, except when the projectile was at the low end of the velocity spectrum (less than 2 km/s). Figure 5 shows the signal from an impact event, in which the projectile did not penetrate the composite plate. The velocity for this impact was 1.8 km/s. The plate in this experiment was the 8-ply IM7/8552 material. The distance of propagation was only 7.2 cm in a direction at a small angle (approximately  $1.5^\circ$ ) from the  $0^\circ$ -fiber direction in this quasi-isotropic material. Again, similar to the signal from high-velocity impact in aluminum, there are large amplitude extensional and flexural mode components. However, the very high-frequency components that were present in Fig. 4a, are missing. This is most likely due to the much higher attenuation at higher frequencies that is typical of composites.

A different result was obtained when the composite plate was penetrated. Figure 6a shows a signal for such a case in the 8-ply material where the projectile velocity was 6.6 km/s. The propagation distance was 14.1 cm in a direction of  $51.4^\circ$  with respect to the  $0^\circ$ -fiber direction. For this signal, the flexural mode component is not present. The signal is composed only of the extensional mode and its reflections from the plate edges. A similar result is shown in Fig. 6b for the 24-ply laminate. The velocity in this case was 5.2 km/s. The propagation distance was 13.0 cm along a  $54.3^\circ$  propagation direction.

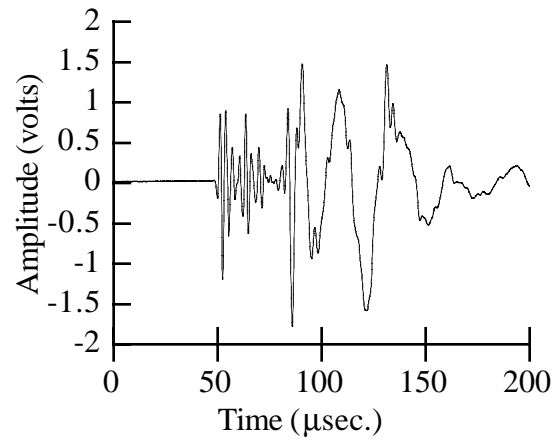


Fig. 5 AE signal produced by non-penetrating high-velocity impact on 8-ply graphite/epoxy composite plate.

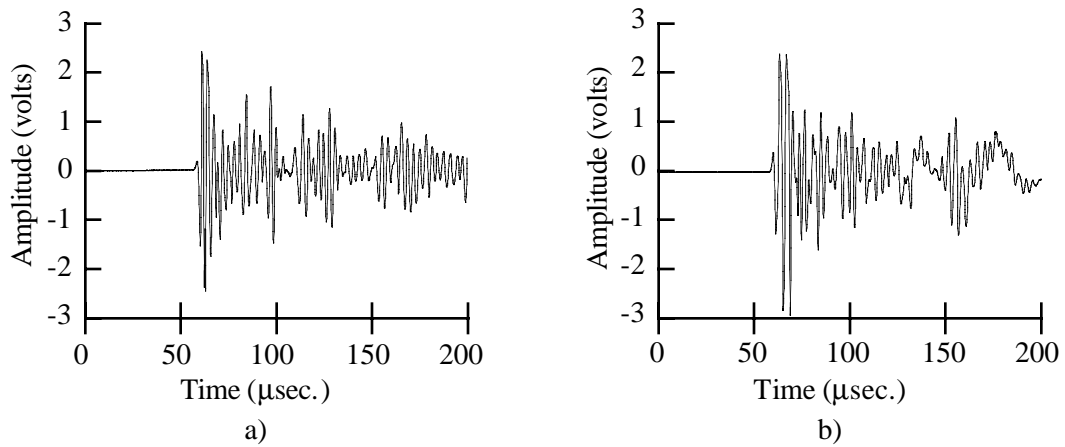


Fig. 6 AE signals produced by penetrating impact in composite plates; a) 8-ply laminate, and b) 24 ply laminate.

#### 4. Summary



In this study, AE signals generated by impact were detected with broadband, high fidelity sensors. A wide variety of impact conditions were studied including both low- and high-velocity impact, and varied impact trajectory in metal and composite targets. In the composite plates at high velocities, both penetrating and non-penetrating impacts were examined. In all cases, the AE signals had very large amplitudes and propagated as plate modes.

AE signals from low- and high-velocity impacts were easily differentiated from their frequency content and modal analysis. Low-velocity impacts produced signals with little extensional mode and large flexural mode components. For variations in velocity over the low-velocity regime, effects on both the amplitude and frequency content of the AE signals were observed. High-velocity, non-penetrating impacts also produced AE signals with large flexural modes. However, these signals had large extensional mode components of comparable amplitude to the flexural mode. The large extensional modes may be due to the in-plane crater deformation caused by impacts at these velocities. When high-velocity impacts fully penetrated the composite plates, the flexural mode was absent from the AE signal. Variations in the impact trajectory had no discernible effect on the modal content of the AE signals at either high or low velocities. The only signal variation was a change in overall amplitude, which was attributed to simple changes in the normal velocity component as a function of impact angle.

These results demonstrate the feasibility for using AE to not only detect and locate impact events on aircraft and spacecraft, but also provide information about the nature of the damage. The very large signal amplitudes for the impacts studied indicate that relatively large sensor spacing might be used for practical, economical, implementation. This, of course, depends on a number of factors such as the minimum allowable undetected impact damage, and the structural complexity of the region to be monitored, which can

significantly affect the propagation of AE waves. The observed variation in signal characteristics with impact parameters such as velocity suggests that quantitative information about the impact parameters could be obtained. Such information could be used to remotely assess damage, which is of particular importance for long-term orbiting spacecraft. Likewise, the ability to differentiate penetrating and non-penetrating impact events would be critical for assessing damage in spacecraft, particularly on pressurized components such as habitat modules and tanks.

However, further study will be necessary to develop and implement a full-scale AE impact-monitoring system for a given application. A wider range of impact velocities, projectile size and materials, and propagation distances, which are representative of those expected for the particular application should be tested. Also, realistic specimen geometry again representative of the aircraft or spacecraft to be monitored should be studied. This will allow the effects of wave propagation such as reflections or attenuation through complex geometry to be evaluated. Such effects can be significant and are often ignored when attempting to extend laboratory AE results to monitor real structures. And finally, as with any AE application, considerable attention needs to be paid to evaluating and eliminating potential noise sources. The development of accurate models to predict AE signals from impact sources will also be of tremendous benefit. Such simulations could help minimize the high expense required for experimentally testing a wide variety of impact conditions, and can be used to help understand and interpret results from actual events.

## **References**

- W. M. Alexander, W. W. McCracken, L. Secretan, and O. E. Berg (1962), "Review of Direct Measurements of Interplanetary Dust from Satellites and Probes," NASA TN D-1669, pp. 39-60.
- W. D. Crozier, and W. Hume (1957), "High Velocity Light Gas Gun," J. Appl. Phys., **28**, 892-894.

- S. K. Datta, T. H. Ju, R. L. Bratton, and A. H. Shah (1992), "Transient Response of a Laminated Composite Plate," *Review of Progress in Quantitative Nondestructive Evaluation*, **11**, 145-151.
- GAO (1990), "Space Program: Space Debris is a Potential Threat to Space Station and Shuttle," GAO Report # GAO/IMTEC-90-18.
- GAO (1992), "Space Station: Delays in Dealing with Space Debris May Reduce Safety and Increase Costs," GAO Report # GAO/IMTEC-92-15.
- D. S. Gardiner and L. H. Pearson (1985), "Acoustic-Emission Monitoring of Composite Damage Occurring Under Static and Impact Loading," *Experimental Techniques*, **9**, 22-28.
- M. R. Gorman (1990), "Plate Wave Acoustic Emission," *J. Acoust. Soc. Am.*, **90**(1), 358-364.
- M. R. Gorman and W. H. Prosser (1991), "AE Source Orientation by Plate Wave Analysis," *Journal of Acoustic Emission*, **9**(4), 283-288.
- I. Kapinsinsky (1978), "On the Reliability of the Acoustic Method of Micrometeoroid Detection," *Bulletin of the Astronomical Institutes of Czechoslovakia*, **29**(6), 326-330.
- M. R. Karim (1991), "Impact Response of a Unidirectional Composite Laminate," *JSME International Journal*, **34**(4), 496-504.
- B. P. Konstantinov, M. M. Bredov, E. P. Mazets, V. N. Panov, R. L. Aptekar, S. V. Golenetskii, Y. G. Guryan, and V. N. Il'inskii, (1969), "Micrometeors in Circumterrestrial Space Observed by Kosmos-163," Translated from *Kosmicheskie Issledovaniya*, **7**(6), 817-821.
- B. M. Lempriere (1989), "Nondestructive Evaluation of Composite Structures in Space," Boeing Report # D180-31598-1.
- A. K. Mal and S. S. Lih (1992), "Wave Field Produced in a Composite Laminate by a Concentrated Surface Force," *Review of Progress in Quantitative Nondestructive Evaluation*, **11**, 137-144.
- F. C. Moon (1973), "Wave Surfaces Due to Impact on Anisotropic Plates," *Journal of Composite Materials*, **7**, 62-79.
- J. M. Nelson and B. M. Lempriere (1987), "Space Station Integrated Wall Design and Penetration Damage Control," Final Report for NASA Contract NAS8-36426.
- E. P. Papadakis (1980), "Broadband Flaw Detection Transducers: Application to Acoustic Emission Pulse Shape and Spectrum Recording Based on Pulse Echo Response Spectrum Corrected for Beam Spreading," *Acoustica*, **46**, 293-298.
- W. H. Prosser (1991), "The Propagation Characteristics of the Plate Modes of Acoustic Emission Waves in Thin Aluminum Plates and Thin Graphite/Epoxy Composite Plates and Tubes," NASA Technical Memorandum 104187.
- E. Schneider and A. Stilp (1990), "Acceleration of Particles in Light Gas Guns for Micrometeoroid/Space Debris Simulation," Proceedings of the International Symposium on Environmental Testing for Space Programs - Test Facilities and Methods, Sponsored by

ESA, Guyenne, T. and Hunt, J., editors, Noordwijk, Netherlands, June 22-29, pp. 385-388.

C. T. Sun and R. Y. S. Lai (1974), "Exact and Approximate Analyses of Transient Wave Propagation in an Anisotropic Plate," *AIAA Journal*, **12**(10), 1415-1417.

N. Takeda, R. L. Sierakowski, and L. E. Malvern (1981), "Wave Propagation Experiments on Ballistically Impacted Composite Laminates," *Journal of Composite Materials*, **15**, 157-174.

D. Weems, H. T. Hahn, E. Granlund, and I. G. Kim (1991), "Impact Detection in Composite Skin Panels Using Piezoelectric Sensors," *American Helicopter Society 47th Annual Forum Proceedings*, **1**, 643-652.